Fish and Shellfish Immunology 92 (2019) 813–820

Contents lists available at ScienceDirect

Fish and Shellfish Immunology

journal homepage: www.elsevier.com/locate/fsi

Full length article

Analysis of the role of IL-10 in the phagocytosis of mIgM$^+$ B lymphocytes in flounder (*Paralichthys olivaceus*)

Shun Yang[a], Xiaoqian Tang[a,b,*], Xiuzhen Sheng[a], Jing Xing[a,b], Wenbin Zhan[a,b]

[a] Laboratory of Pathology and Immunology of Aquatic Animals, KLMME, Ocean University of China, 5 Yushan Road, Qingdao, 266003, China
[b] Laboratory for Marine Fisheries Science and Food Production Processes, Qingdao National Laboratory for Marine Science and Technology, Qingdao, 266071, China

ARTICLE INFO

Keywords:
Phagocytosis
mIgM$^+$ B lymphocytes
Interleukin-10
Stat3
Paralichthys olivaceus

ABSTRACT

B cells have been found to have phagocytic activity in recent years, but the studies exploring the regulation mechanisms are still lacking to date. In the present study, the recombinant interleukin-10 (rIL-10) was obtained to study the function of IL-10 on phagocytosis of flounder (*Paralichthys olivaceus*) mIgM$^+$ B lymphocytes. Flow cytometric analysis showed that IL-10 significantly enhanced the phagocytosis of *Edwardsiella tarda* but not *Lactococcus lactis* by mIgM$^+$ B lymphocytes. Moreover, significantly higher intracellular ROS levels were detected in mIgM$^+$ B lymphocytes following rIL-10 stimulation. The qRT-PCR analysis showed that rIL-10 could upregulate the expressions of *IL*-10Rb and *Stat3* in mIgM$^+$ B lymphocytes, suggesting that IL-10 might modulate the phagocytosis of mIgM$^+$ B lymphocytes by activating IL-10R and Stat3. In addition, we also found that the enhancing effect of IL-10 on phagocytosis and intracellular ROS levels of mIgM$^+$ B lymphocytes were suppressed by the administration of niclosamide. These results collectively demonstrated that IL-10 enhanced mIgM$^+$ B lymphocyte-mediated phagocytosis of *E. tarda* and intracellular bactericidal ability, and IL-10R and Stat3 might play a curial role in the regulation of IL-10-stimulated phagocytosis, which would deepen our understanding of regulation mechanism of B cell phagocytosis.

1. Introduction

The immune system of fish is comprised of two immunity strategies, including adaptive and innate immunity. The innate immune system, as an old evolutionary defense strategy, represents the first line of defense against pathogenic organisms and other foreign materials, and also plays an important role in driving adaptive immunity [1]. Phagocytosis is the uptake by the cell of diverse particulate targets, which plays an important role in several biological processes such as bacterial killing and antigen cross-presentation [2,3]. Phagocytosis in mammals is mainly performed by the professional phagocytes, such as macrophages, neutrophils and dendritic cells (DCs) [4]. However, accumulating evidences have demonstrated that B cells in fish also possess potent phagocytic ability like macrophages [5–9]. It has been found that B cells could phagocytose microspheres and bacteria in many fish species, such as rainbow trout (*Oncorhynchus mykiss*) [5], half-smooth tongue sole (*Cynoglossus semilaevis*) [8] and sea bass (*Lateolabrax japonicus*) [9]. Moreover, the B cells originating from amphibians (e.g. *Xenopus laevis*) and reptiles (e.g. *Trachemys scripta*) were also found to possess phagocytic activity [5,10]. It was also reported that human Raji B-cell line have the abilities to engulf both live and dead *Mycobacterium tuberculosis* [11]. In mouse, B1 cells that constitute innate B cell subset were found to have the abilities to engulf microspheres and bacteria, whereas the phagocytic capacity was lost in conventional B2 cells [12,13]. These studies collectively suggested that the phagocytic capacity of B cells seems to be an ancient trait of innate B cells that has been well maintained in early vertebrates. However, the studies on regulation mechanism of B cell phagocytosis are still lacking.

Interleukin 10 (IL-10), an important anti-inflammatory mediator, is produced by many immune cell types, such as macrophages, B cells and DCs [14]. In mammals, IL-10 binds with high affinity to IL-10 receptor (IL-10R), triggering STAT3 phosphorylation, dimerization, and translocation to the nucleus, thereby modulating the inflammatory response [14,15]. It has been reported that anti-inflammatory macrophages with high phagocytic capacity aslo secreted high level of IL10 [16]. Previous studies also indicated that IL-10 can trigger macrophage polarization toward an alternatively activated anti-inflammatory, immune-regulatory, or tissue remodeling M2 phenotype [17–19]. In human, IL-10 has been shown to increase human peripheral blood macrophage to phagocytose non-bone associated apoptotic cells [20,21]. However, it

* Corresponding author. Laboratory of Pathology and Immunology of Aquatic Animals, KLMME, Ocean University of China, 5 Yushan Road, Qingdao, 266003, China.
E-mail address: tangxq@ouc.edu.cn (X. Tang).

https://doi.org/10.1016/j.fsi.2019.06.059
Received 10 April 2019; Received in revised form 28 June 2019; Accepted 30 June 2019
Available online 01 July 2019

has not yet been determined whether in teleost the phagocytic capacity of B cells is regulated by IL-10.

In addition, intracellular ROS include superoxide anion (O_2^-), singlet oxygen (O_2), hydrogen peroxide (H_2O_2), and hydroxyl radicals (OH^-), which has been regarded as excellent indicators for cells bactericidal ability [22]. Mitochondrial ROS also contribute to macrophage bactericidal activity which is critical for protection against microorganisms [23]. Previous studies have shown that the hydrogen peroxide is by itself microbicidal, which can also further react in several ways with other components that also have potent microbicidal abilities, such as myeloperoxidase, to form hypocloride ions (OCl^-) and singlet oxygen ($^*O_2$) [24,25]. Moreover, the respiratory burst is regarded as a potent response in phagocytic cells, which also contributes to innate immunity through generation of intracellular ROS mediated by the multicomponent enzyme NADPH oxidase [26,27]. Therefore, the intracellular ROS activity can be used as indicator to evaluate the bactericidal ability of phagocytes.

In the present study, flounder IL-10 was recombinantly expressed using pET-28a vector. Then the effect of IL-10 on phagocytosis and intracellular ROS activity of $mIgM^+$ B lymphocytes was analyzed by flow cytometry. Moreover, $mIgM^+$ B lymphocytes were sorted using MAb against IgM, and the changes in mRNA expression of *NOD-like receptor C* (*NLRC*), *scavenger receptor class F member 1* (*Scarf1*), *TLR1*, *IL*-10Rb and *Stat3* in $mIgM^+$ B lymphocytes were detected by quantitative real-time PCR (qRT-PCR) following rIL-10 stimulation. Furthermore, the role of Stat3 in IL-10 regulation of phagocytosis of $mIgM^+$ B lymphocytes was also analyzed by niclosamide treatment. This work establishes a role of IL-10 on the phagocytic capacity of $mIgM^+$ B lymphocytes, contributing to a deeper understanding of how B cell phagocytosis is regulated in teleost.

2. Materials and methods

2.1. Fish

Flounders (750 ± 50 g) were purchased from a fish farm in Rizhao, Shandong Province, PR China. The fish were maintained in tanks containing aerated sand-filtered seawater at 20 ± 0.5 °C for one week prior to experiments.

2.2. Expression and purification of rIL-10

The domains of IL-10 (Genbank No. AB685381.1) were analyzed using SMART program. Then, specific primers (Table 1) were designed to amplify the sequences encoding IL-10 excluding the region coding for its signal peptide by RT-PCR. The PCR products were purified and digested with specific restriction enzymes, and then ligated into pET-28a vector to construct recombinant plasmid pET-28a-IL-10. The recombinant plasmids were transformed into *E. coli* (DE3), then positive transformant was screened by colony PCR and fragment sequencing. The transformant was cultured in LB medium to mid-logarithmic phase and induced by adding isopropyl β-D-1-thiogalactopyranoside. His-tagged rIL-10 was purified using His TrapTM HP Ni-Agarose (GE Healthcare China, Beijing, China) followed by the manufacturer's instruction. For refolding, the purified rIL-10 was conducted by the stepwise dialysis method as previously described [28]. Then, the purified and refolded proteins were treated with Triton X-114 to remove endotoxin and assessed by SDS-PAGE. The residual endotoxin within the recombinant protein preparation was detected using the ToxinSensorTM Chromogenic LAL Endotoxin Assay Kit (GenScript, China). The concentrations of proteins were determined using the Bradford method.

Table 1
Detailed information of primers used in this study.

Primer no	Primer name	Primer sequence (5′-3′)
1	*IL-10*-F	CCGGAATTCAGTCCCATGTGTAATAACCA (EcoR I)
2	*IL-10*-R	ACGCGTCGACGGTGGAGGTTGCATGGTTTT (Sal I)
3	*Scarf1*-F	AAGGGAGTCGAGGGGATC
4	*Scarf1*-R	CGTCTTATAGGTTTACAAATGGC
5	*NLRC*-F	GGTCATTTCATCGCTTATCA
6	*NLRC*-R	AAAGAAAGACAGCGTGCC
7	*TLR1*-F	TCCGCACTTCTCATCTTTAT
8	*TLR1*-R	ATTTCACCACAGCCCTTC
9	*IL*-10Rb-F	CACCATCACTGCCTTCGT
10	*IL*-10Rb-R	GGTTGTTGGATACCCCTTT
11	*Stat3*-F	TGGCACTGTGGAATGAGG
12	*Stat3*-R	TGTAGGGCTCCACCGACT
13	*18S rRNA*-F	GGTCTGTGATGCCCTTAGATGTC
14	*18S rRNA*-R	AGTGGGGTTCAGCGGGTTAC

Note: Nucleotides underlined indicate restriction sites used for cloning.

2.3. Cell sorting

The flounder $mIgM^+$ B lymphocytes were sorted from peripheral blood using immunomagnetic bead method as previously described with some modifications [29]. Briefly, the leukocytes isolated from peripheral blood were incubated with MAb against IgM, produced previously in our laboratory [30], at 22 °C for 1.5 h, then washed three times using magnetic activated cell sorting (MACS) buffer (PBS containing 2 mM EDTA and 0.5% bovine serum albumin (BSA)). Then leukocytes were suspended in MACS buffer (80 μl per 10^7 cells) and incubated with goat anti-mouse IgG magnetic beads (20 μl per 10^7 cells, Miltenyi Biotec, Germany) for 15 min at 4 °C, then washed again. The leukocytes were suspended in MACS buffer (500 μl per 10^8 cells) and filtered through a 40 μm nylon mesh. A MACS LS column (Miltenyi Biotech) was installed in MACS separator according to the manufacturer's instructions and balanced with 3 ml MACS buffer. Then the leukocytes suspension flowed through the column, and the magnetically unlabeled leukocytes were wasted off using MACS buffer. Then MACS LS column was removed from MACS separator, and the magnetically labeled leukocytes were collected using MACS buffer. For obtaining high purity $mIgM^+$ B lymphocytes, the magnetically labeled leukocytes were secondary sorted using new balanced MACS LS columns (Miltenyi Biotech, Germany) as previously described. The purity of sorted $mIgM^+$ B lymphocytes were analyzed by flow cytometry and Indirect immunofluorescence assay (IIFA).

2.4. rIL-10 stimulation assay

The leukocytes were isolated from the flounder peripheral blood using discontinuous percoll (Pharmacia) gradient (1.020/1.070) according to the method described by Li et al. [30]. Then isolated leukocytes were suspended in serum-free L-15 medium, and transferred to 24-well culture plates (500 μl/well) to ensure 5×10^6 cells per well. The leukocytes were next incubated with flounder rIL-10 (0.25 μg/well, at a final concentration of 0.5 μg/ml) for 12 h at 22 °C. The his-tag protein of pET-28a vector instead of rIL-10 was used as negative control. After incubation, the leukocytes were collected for phagocytosis assay, intracellular ROS detection and qRT-PCR analysis.

2.5. Niclosamide inhibition assay

The leukocytes isolated from flounder peripheral blood were suspended in serum-free L-15 medium. Then isolated leukocytes were transferred to 24-well culture plates (500 μl/well) to ensure 5×10^6 cells per well. The leukocytes in each well were incubated with 10 μM niclosamide (Selleck, USA) for 2 h, with DMF administered to the control samples. Next, the leukocytes were incubated with rIL-10 (0.25 μg/well, at a final concentration of 0.5 μg/ml) for 12 h at 22 °C. The his-tag protein of pET-28a vector instead of rIL-10 was used as control. Then the leukocytes were collected for phagocytosis assay and

intracellular ROS detection.

2.6. Phagocytosis assay

For the phagocytosis assay, *Lactococcus lactis* and *Edwardsiella tarda* were labeled with FITC as previously described [9]. Then phagocytosis assay was performed as previously described with some modification [9]. Briefly, the leukocytes in serum-free L-15 medium were counted and diluted to 1×10^7 cells/ml. Following the addition of FITC-labeled *L. lactis* or *E. tarda*, 500 μl of the leukocyte suspension was added into the wells of a 24-well culture plate at a cell to bacteria ratio of 1:20, and then incubated for 1 h at 22 °C. After incubation, the non-ingested *L. lactis* were removed by placing the cell suspension on top of a 1.077 percoll gradient and centrifugation at 680*g* for 10 min at 4 °C. Non-ingested *E. tarda* were removed by placing the cell suspensions on top of a glucose cushion (3 ml PBS, pH 7.3, with 3% (w/v) BSA and 4.5% (w/v) D-glucose) and centrifugation at 100*g* for 10 min at 4 °C. Then the collected cells were stained with MAb specific for flounder IgM, produced previously in our laboratory [30]. Following washing with PBS, the cells were labeled with Alexa Fluor® 647 goat anti-mouse IgG (Invitrogen, USA) and then analyzed using BD Accuri C6 Flow Cytometer. Finally, the mIgM$^+$ B lymphocytes were gated for the analysis of phagocytosis.

2.7. Flow cytometry analysis of intracellular ROS in mIgM$^+$ B lymphocytes

The leukocytes were incubated with MAb specific for flounder IgM at 22 °C for 1.5 h. After washing with PBS, the cells were labeled with Alexa Fluor® 647 goat anti-mouse IgG (Invitrogen, Molecular Probes) for 45 min at 4 °C. Finally, intracellular ROS was detected by reactive oxygen species assay kit (Beyotime, China) according to the manufacturer's instructions with some modification. Briefly, the cells were cultured in serum-free L-15 medium containing 0.1% DCFH-DA at 22 °C for 30 min, prior to being washed with serum-free L-15 medium three times and acquired on the BD Accuri C6 flow cytometer. The fluorescence intensity of DCFH-DA was detected to assess intracellular mIgM$^+$ B lymphocyte ROS levels.

2.8. Quantitative real-time PCR

For qRT-PCR, the mIgM$^+$ B lymphocytes were sorted form the pooled peripheral blood of four fish as mentioned above. Then total RNA was extracted from mIgM$^+$ B lymphocytes using the RNeasy Plus Mini Kit (Qiagen, USA) following the manufacturer's instruction. After checking the quality of RNA using a Bioanalyzer 2100 (Agilent Technologies, USA), the first-strand cDNA was synthesized using the SuperScript® III RT kit (Invitrogen, USA) and diluted to 50 ng/μl for qRT-PCR. The qRT-PCR was carried out using SYBR GreenIMaster (Roche, CH) in a LightCycler® 480 II Real Time System (Roche, CH). Each assay was performed in triplicate with the *18s rRNA* gene as the internal reference. All data were analyzed relative to the *18s rRNA* gene by the $2^{-\triangle\triangle Ct}$ method [31]. The differences between the IL-10-stimulated and control groups were employed to assess changes in genes expression. The primers for *Scarf1*, *NLRC*, *TLR1*, *IL*-10Rb and *Stat3* were designed according to the corresponding sequences and listed in Table 1.

2.9. Statistical analysis

The statistical analysis was performed using statistical product and service solution (SPSS) software (Version 20.0; SPSS, Inc), and statistical significance was analyzed with independent-samples *t*-test and duncan's multiple range test (DMRT), respectively. The results were given as mean ± S.D., and differences were considered significant when $p < 0.05$.

3. Results

3.1. Expression and purification of rIL-10

Based on the SMART program analysis, the flounder IL-10 excluding the region coding for its signal peptide (amino acid residue position 1–22) was expressed using *E. coli* (DE3) with pET-28a vector (Fig. S1A). SDS-PAGE analysis showed that a distinct band representing about 26 kDa was observed after IPTG induction, which was consistent with the predicted molecular mass of flounder IL-10 plus his-tag protein of pET-28a vector, suggesting that the IL-10 was successfully expressed (Fig. S1B). After purification with the $Ni2^+$ affinity chromatography and refolding with the stepwise dialysis method, the high purity rIL-10 protein were obtained (Fig. S1B). After Triton X-114 treatment, the endotoxin content was < 0.05 endotoxin units per mg of purified rIL-10.

3.2. The effects of IL-10 on the phagocytosis by mIgM$^+$ B lymphocytes

For the phagocytosis assay, *L. lactis* and *E. tarda* were labeled with FITC, and flow cytometry and fluorescence microscopy analysis showed that all *L. lactis* and *E. tarda* were successfully labeled with FITC and could be used for further analysis of phagocytosis (Figs. S3 and S4). Then the changes of phagocytosis by mIgM$^+$ B lymphocytes were detected by flow cytometry upon rIL-10 stimulation. The results showed that the phagocytic rate of *L. lactis* by mIgM$^+$ B lymphocytes had no significant change following rIL-10 stimulation (Fig. 1A). In contrast, significantly higher phagocytic rate of *E. tarda* by mIgM$^+$ B lymphocytes was detected to be 55.3 ± 3.23% following rIL-10 stimulation, compared with control group of 42.0 ± 2.62% (Fig. 1B).

3.3. The effects of IL-10 on the intracellular ROS activity by mIgM$^+$ B lymphocytes

Following rIL-10 stimulation, the intracellular ROS levels of mIgM$^+$ B lymphocytes were analyzed using ROS assay kit by flow cytometry. Based on the DCFH-DA fluorescence intensity, the mIgM$^+$ B lymphocytes of flounder could be subdivided into two distinct populations with high and low intracellular ROS levels, respectively. When the cells were treated with the his-tag protein, 16 ± 1.4% mIgM$^+$ B lymphocytes had high intracellular ROS levels. In comparison, rIL-10 treatment significantly enhanced ROS production, and 31.2 ± 2.0% mIgM$^+$ B lymphocytes displayed high intracellular ROS levels (Fig. 2).

3.4. Expression of immune-related genes following IL-10 stimulation

The results of flow cytometry and IIFA demonstrated that high purity of mIgM$^+$ B lymphocytes were obtained by immunomagnetic bead method (Fig. S2). Then the changes in the expressions of *NLRC*, *Scarf1*, *TLR1*, *IL*-10Rb and *Stat3* mRNA in mIgM$^+$ B lymphocytes were analyzed by qRT-PCR, following rIL-10 stimulation. The qRT-PCR analysis showed that rIL-10 induce the up-regulation of *NLRC* and *Scarf1* in mIgM$^+$ B lymphocytes, but inhibited *TLR1* expression (Fig. 3). Moreover, the results showed that the expressions of *IL*-10RB and *Stat3* in mIgM$^+$ B lymphocytes were up-regulated following rIL-10 stimulation (Fig. 3).

3.5. The role of Stat3 in the IL-10-stimulated regulation of mIgM$^+$ B lymphocyte phagocytosis

To investigate the role of Stat3 in the IL-10-stimulated regulation of mIgM$^+$ B lymphocyte phagocytosis, niclosamide was employed to inhibit Stat3 phosphorylation. In the presence of niclosamide alone, slightly lower phagocytic rate of 39.9 ± 1.55% was observed compared with control group but no significant difference. After treatment with rIL-10 alone, 57.3 ± 2.46% mIgM$^+$ B lymphocytes were able to

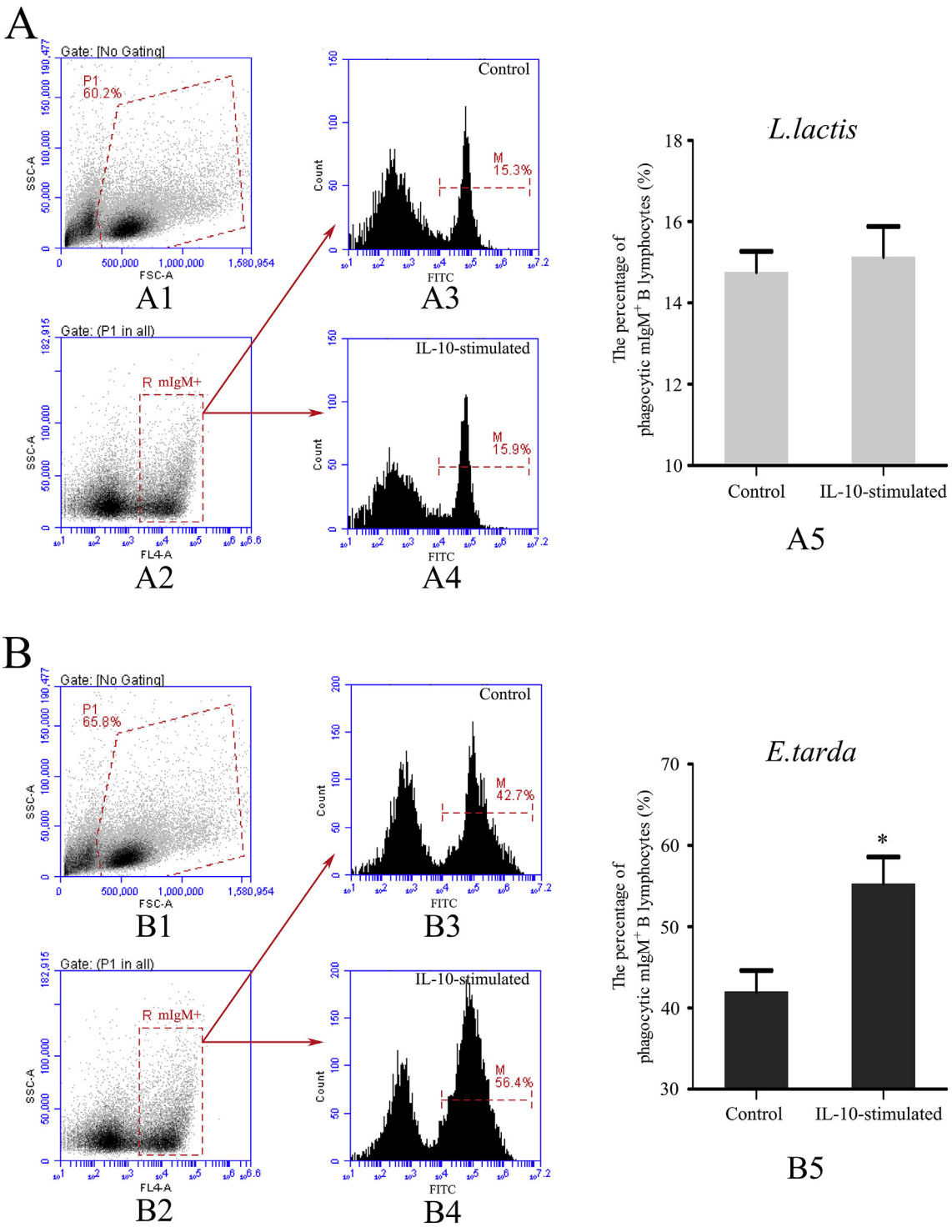

Fig. 1. Flow cytometric analysis of the phagocytosis by mIgM$^+$ B lymphocytes with rIL-10 stimulation. **(A, B)** Phagocytosis of *L. lactis* **(A)** and *E. tarda* **(B)** by mIgM$^+$ B lymphocytes with rIL-10 stimulation. Leukocytes in the peripheral blood were gated (P1) on FSC/SSC dot plot **(A1, B1),** then mIgM$^+$ B lymphocytes were gated (R) for analysis of phagocytosis **(A2, B2)**. The fluorescence histogram showing percentages of phagocytic mIgM$^+$ B lymphocytes (scale of M) in control group **(A3, B3)** and IL-10-stimulated group **(A4, B4)**. The data of phagocytic rates of *L. lactis* **(A5)** and *E. tarda* **(B5)** by mIgM$^+$ B lymphocytes with rIL-10 stimulation was analyzed using SPSS software, respectively (mean ± S.D., n = 3); the asterisk on the bars represents statistical significance of phagocytic rates compared with control groups. ($p < 0.05$).

phagocytose *E. tarda*. However, significantly lower phagocytic rate of 46.4 ± 1.76% was observed in the presence of rIL-10 and niclosamide, compared with treatment with rIL-10 alone (Fig. 4). Similarly, only slightly lower percentage of mIgM$^+$ B lymphocytes with high intracellular ROS levels of 15.1 ± 1.10% was observed but no significant difference in the presence of niclosamide alone, compared to control group. However, the intracellular ROS levels of rIL-10-stimulated mIgM$^+$ B lymphocytes were significantly decreased following niclosamide treatment, and the percentage of mIgM$^+$ B lymphocytes with high intracellular ROS levels was decreased from 31.9 ± 1.70% to 22.8 ± 1.52% (Fig. 5).

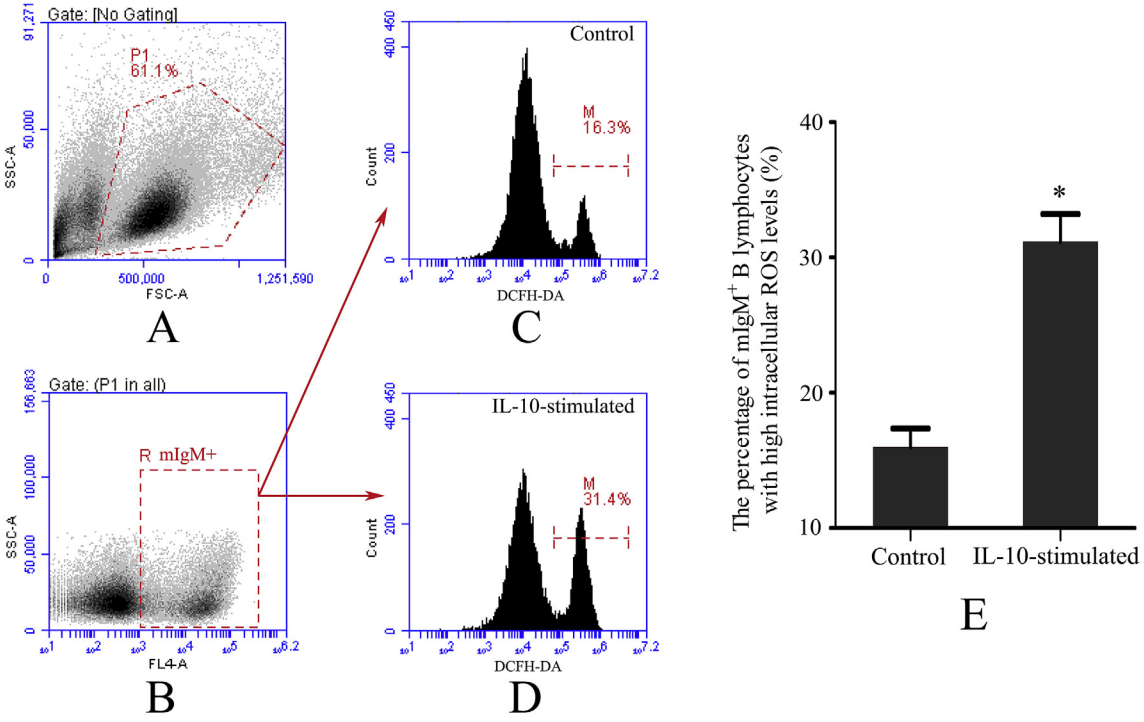

Fig. 2. Flow cytometric analysis of intracellular ROS activity of mIgM$^+$ B lymphocytes with rIL-10 stimulation. Leukocytes in the peripheral blood were gated (P1) on FSC/SSC dot plot **(A),** then mIgM$^+$ B lymphocytes were gated (R) for analysis of intracellular ROS levels **(B)**. The fluorescence histogram showing the percentage of mIgM$^+$ B lymphocytes with high intracellular ROS levels (scale of M) in control group **(C)** and IL-10-stimulated group **(D)**. The data of percentage of mIgM$^+$ B lymphocytes with high intracellular ROS levels with rIL-10 stimulation **(E)** were analyzed using SPSS software (mean ± S.D., n = 3); the asterisk on the bars represents statistical significance of intracellular ROS levels compared with control group. ($p < 0.05$).

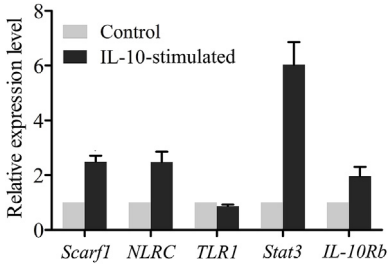

Fig. 3. The qRT-PCR analysis of the expression of several immune-related genes in mIgM$^+$ B lymphocytes with rIL-10 stimulation. The mRNA levels of each immune-related gene were normalized to those of *18S rRNA*; For each gene, the mRNA level of the control group was set as 1. Error bars represent the standard deviation of three technical replicates from a pool of sorted mIgM$^+$ lymphocytes.

4. Discussion

B cell, as primary effector in humoral immunity, play an important role in immune response by antigen presentation and antibody secretion, which have long been thought to lack phagocytic activity [4,32]. However, recent accumulating studies have shown that B cells also possess phagocytic ability in teleosts, amphibians, reptiles and mammals [5–13]. Previous studies also shows that B cells could initiate the adaptive immune response by destroying the internalized bacteria and presenting processed antigens to CD4$^+$ T cells, following phagocytosis [33,34]. These finding inspire us to further explore the function of B cells in phagocytosis. IL-10 is an important anti-inflammatory mediator, which could modulate the phagocytosis of macrophages [14,20,21]. In this study, we found that rIL10 enhanced the ability of flounder mIgM$^+$ B lymphocytes to phagocytose *E. tarda* but not *L. lactis*. The pattern recognition receptors (PRRs) can recognize microbial pathogens by identifying the pathogen-associated molecular patterns (PAMPs), playing a vital role in triggering phagocytosis to clear microbial pathogens [35]. Pervious studies have been shown that IL-10 can modestly activated CD14 antigen expression, and augments phagocytic capacity of human mononuclear phagocytes [36]. In the present study, qRT-PCR analysis showed that IL-10 induced an up-regulated expression of *NLRC* and *Scarf1* in mIgM$^+$ B lymphocytes, but inhibited *TLR1* expression, which indicated that IL-10 has different regulatory effects on different PRRs. Previous studies have been shown that different PRRs recognize different PAMPs on microbial pathogens [37–40]. Therefore, we speculated that IL-10 regulate the phagocytosis of mIgM$^+$ B lymphocytes by modulating the expression of PRRs, and the difference in IL-10 regulation of B cell phagocytosis to *L. lactis* and *E. tarda* might be caused by the different effects of IL-10 on PRRs.

Intracellular ROS is excellent indicators for cells bactericidal ability, and previous studies have shown that the hydrogen peroxide, the main component of intracellular ROS, also possessed the microbicidal effect by itself [22,24,25]. Moreover, the respiratory burst is an non-specific and microbicide defense mechanism of phagocytic cells, which also contributes to innate immunity through generation of intracellular ROS mediated by the multicomponent enzyme NADPH oxidase [26,27]. In this study, we found that IL-10 enhanced the intracellular ROS levels of mIgM$^+$ B lymphocytes, which indicated that IL-10 could also enhance the intracellular bactericidal ability of mIgM$^+$ B lymphocytes. These evidences collectively demonstrated that IL-10 can modulate mIgM$^+$ B lymphocytes-mediated phagocytosis, enhancing their phagocytic and intracellular bactericidal ability.

In mammals, IL-10 modulate the immune response by activating IL-10R, then triggering Stat3 phosphorylation, dimerization, and translocation to the nucleus [14,15]. Previous studies have been shown that IL-10-Stat3 signaling pathway play an important role in promoting alternative macrophage activation [41,42]. Moreover, it also has been reported that paeoniflorin can modulate the microglia inflammation and phagocytosis through activating of IL-10-Stat3 signaling pathway [43]. In the present study, IL-10Rb and Stat3 were found to be upregulated

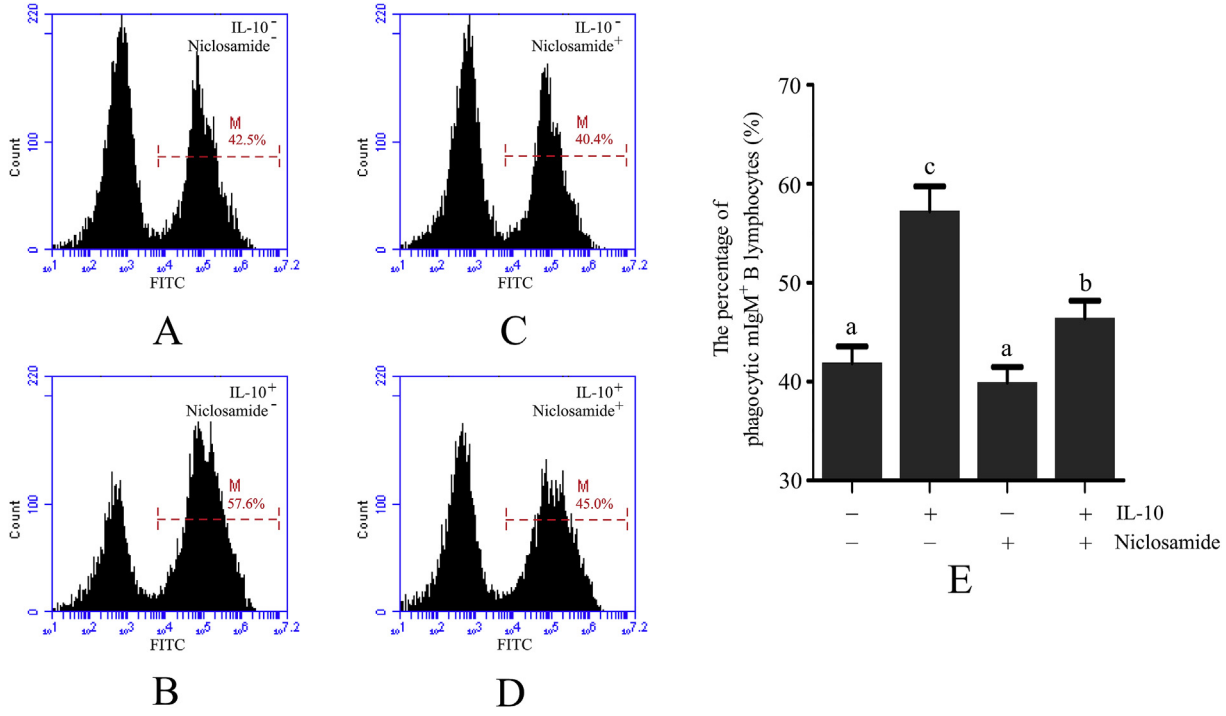

Fig. 4. Flow cytometric analysis of phagocytosis of *E. tarda* by mIgM$^+$ B lymphocytes with combination treatment of IL-10 and niclosamide. The fluorescence histogram showing the percentages of phagocytic mIgM$^+$ B lymphocytes (scale of M) in control group **(A)**, IL-10-stimulated group **(B)**, niclosamide-treated group **(C)** and combination of IL10 and niclosamide-treated group **(D)**. The data of phagocytic rates of *E. tarda* by mIgM$^+$ B lymphocytes with combination treatment of IL-10 and niclosamide **(E)** was analyzed using SPSS software (mean ± S.D., n = 3); different capital letters on the bars represents statistical significance of phagocytic rates among different treated groups. ($p < 0.05$).

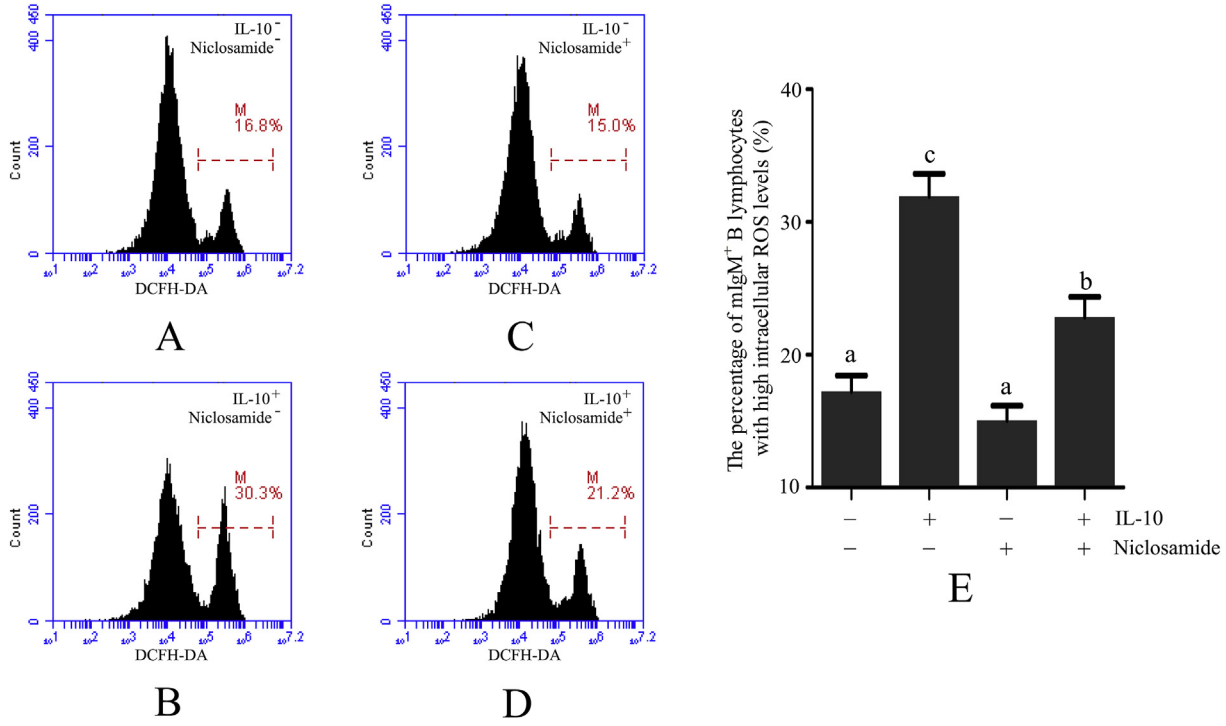

Fig. 5. Flow cytometric analysis of intracellular ROS activity in mIgM$^+$ B lymphocytes with combination treatment of IL-10 and niclosamide. The fluorescence histogram showing the percentage of mIgM$^+$ B lymphocytes with high intracellular ROS levels (scale of M) in control group **(A)**, IL-10-stimulated group **(B)**, niclosamide-treated group **(C)** and combination of IL10 and niclosamide-treated group **(D)**. The data of percentage of mIgM$^+$ B lymphocytes with high intracellular ROS levels with niclosamide combination treatment of IL-10 and niclosamide **(E)** was analyzed using SPSS software (mean ± S.D., n = 3); different capital letters on the bars represents statistical significance of intracellular ROS levels among different treated groups. ($p < 0.05$).

upon IL-10 stimulation in the flounder mIgM$^+$ B lymphocytes. Moreover, flow cytometric analysis showed that the enhancement effect of IL-10 on the phagocytic and intracellular ROS activity of mIgM$^+$ B lymphocytes could be suppressed by the administration of niclosamide. As an inhibitor of Stat3 phosphorylation, niclosamide is routinely used to study the function of Stat3 in many settings [44–46]. We speculated that Stat3 may be implicated in the regulation of IL-10-stimulated phagocytosis in flounder mIgM$^+$ B lymphocytes. In addition, the results showed that niclosamide also had a slight impact on phagocytosis and intracellular ROS activity of mIgM$^+$ B lymphocytes. Thus, further studies are needed to improve our understanding the role of Stat3 in the regulatory effect of IL-10 on mIgM$^+$ B lymphocyte-mediated phagocytosis.

In conclusion, our findings suggest that IL-10 enhances the phagocytic ability of mIgM$^+$ B lymphocytes to ingest *E. tarda* but not *L. lactis*. Moreover, we also found that IL-10 enhances the intracellular ROS levels of mIgM$^+$ B lymphocytes. Further analysis speculates that IL-10R and Stat3 might potentially play an important role in the regulation of IL-10-stimulated phagocytosis in flounder mIgM$^+$ B lymphocytes. We envisage that this research will deepen our understanding of the mechanisms underlying the regulation of B cell phagocytosis.

Acknowledgements

This study was supported by the National Natural Science Foundation of China (31730101; 31872590; 31672685; 31672684; 31472295), Natural Science Foundation of Shandong Province (ZR2019MC029), National key Research and Development Program of China (2018YFD0900503), the Fundamental Research Funds for the Central Universities (201822015) and Taishan Scholar Program of Shandong Province.

Appendix A. Supplementary data

Supplementary data to this article can be found online at https://doi.org/10.1016/j.fsi.2019.06.059.

References

[1] S.K. Whyte, The innate immune response of finfish–a review of current knowledge, Fish Shellfish Immunol. 23 (2007) 1127–1151.
[2] M. Desjardins, M. Houde, E. Gagnon, Phagocytosis: the convoluted way from nutrition to adaptive immunity, Immunol. Rev. 207 (2005) 158–165.
[3] L.M. Stuart, R.A.B. Ezekowitz, Phagocytosis: elegant complexity, Immunity 22 (2005) 539–550.
[4] M. Rabinovitch, Professional and non-professional phagocytes: an introduction, Trends Cell Biol. 5 (1995) 85–87.
[5] J. Li, D.R. Barreda, Y.A. Zhang, H. Boshra, A.E. Gelman, S. LaPatra, L. Tort, J.O. Sunyer, B lymphocytes from early vertebrates have potent phagocytic and microbicidal abilities, Nat. Immunol. 7 (2006) 1116–1124.
[6] H.S. Øverland, E.F. Pettersen, A. Rønneseth, H.I. Wergeland, Phagocytosis by B-cells and neutrophils in Atlantic salmon (*Salmo salar* L.) and Atlantic cod (*Gadus morhua* L.), Fish Shellfish Immunol. 28 (2010) 193–204.
[7] A. Rønneseth, D.B. Ghebretnsae, H.I. Wergeland, G.T. Haugland, Functional characterization of IgM$^+$ B cells and adaptive immunity in lumpfish (*Cyclopterus lumpus* L.), Dev. Comp. Immunol. 52 (2015) 132–143.
[8] S. Yang, X. Tang, X. Sheng, J. Xing, W. Zhan, Development of monoclonal antibodies against IgM of half-smooth tongue sole (*Cynoglossus semilaevis*) and analysis of phagocytosis of fluorescence microspheres by mIgM+ lymphocytes, Fish Shellfish Immunol. 66 (2017) 280–288.
[9] S. Yang, X. Tang, X. Sheng, J. Xing, W. Zhan, Development of monoclonal antibodies against IgM of sea bass (*Lateolabrax japonicus*) and analysis of phagocytosis by mIgM+ lymphocytes, Fish Shellfish Immunol. 78 (2018) 372–382.
[10] L.M. Zimmerman, L.A. Vogel, K.A. Edwards, R.M. Bowden, Phagocytic B Cells in a Reptile Phagocytic B Cells in a Reptile, Society, 2010, pp. 270–273.
[11] Q. Zhu, M. Zhang, M. Shi, Y. Liu, Q. Zhao, W. Wang, G. Zhang, L. Yang, J. Zhi, L. Zhang, G. Hu, P. Chen, Y. Yang, W. Dai, T. Liu, Y. He, G. Feng, G. Zhao, Human B cells have an active phagocytic capability and undergo immune activation upon phagocytosis of *Mycobacterium tuberculosis*, Immunobiology 221 (2016) 558–567.
[12] D. Parra, A.M. Rieger, J. Li, Y.-A. Zhang, L.M. Randall, C.A. Hunter, D.R. Barreda, J.O. Sunyer, Pivotal advance: peritoneal cavity B-1 B cells have phagocytic and microbicidal capacities and present phagocytosed antigen to CD4+ T cells, J. Leukoc. Biol. 91 (2012) 525–536.
[13] M. Nakashima, M. Kinoshita, H. Nakashima, Y. Habu, H. Miyazaki, S. Shono, S. Hiroi, N. Shinomiya, K. Nakanishi, S. Seki, Pivotal Advance: characterization of mouse liver phagocytic B cells in innate immunity, J. Leukoc. Biol. 91 (2012) 537–546.
[14] K.G. Schmetterer, W.F. Pickl, The IL–10/STAT3 axis: contributions to immune tolerance by thymus and peripherally derived regulatory T-cells, Eur. J. Immunol. 47 (2017) 1256–1265.
[15] M.N. Michalski, A.J. Koh, S. Weidner, H. Roca, L.K. McCauley, Modulation of osteoblastic cell efferocytosis by bone marrow macrophages, J. Cell. Biochem. (2016) 2697–2706.
[16] N. Dam, H.R. Hocine, I. Palacios, O. DelaRosa, R. Menta, D. Charron, A. Bensussan, H. El Costa, N. Jabrane-Ferrat, W. Dalemans, E. Lombardo, R. Al-Daccak, Human cardiac-derived stem/progenitor cells fine-tune monocyte-derived descendants activities toward cardiac repair, Front. Immunol. 8 (2017) 1–16.
[17] F.O. Martinez, S. Gordon, The M1 and M2 paradigm of macrophage activation: time for reassessment, F1000Prime Rep. 6 (2014) 1–13.
[18] A. Sica, A. Mantovani, Macrophage plasticity and polarization: in vivo veritas, J. Clin. Investig. 122 (2012) 787–795.
[19] F. Rey-Giraud, M. Hafner, C.H. Ries, In vitro generation of monocyte-derived macrophages under serum-free conditions improves their tumor promoting functions, PLoS One 7 (2012).
[20] M. Lingnau, C. Höflich, H.D. Volk, R. Sabat, W.D. Döcke, Interleukin-10 enhances the CD14-dependent phagocytosis of bacteria and apoptotic cells by human monocytes, Hum. Immunol. 68 (2007) 730–738.
[21] C.A. Ogden, J.D. Pound, B.K. Batth, S. Owens, I. Johannessen, K. Wood, C.D. Gregory, Enhanced apoptotic cell clearance capacity and B cell survival factor production by IL-10-activated macrophages: implications for burkitt's lymphoma, J. Immunol. 174 (2005) 3015–3023.
[22] C.E. Covantes-Rosales, A.M. Trujillo-Lepe, K.J.G. Diaz-Resendiz, G.A. Toledo-Ibarra, G.H. Ventura-Ramon, P.C. Ortiz-Lazareno, et al., Phagocytosis and ROS production as biomarkers in Nile tilapia (Oreochromis niloticus) leukocytes by exposure to organophosphorus pesticides, Fish Shellfish Immunol. 84 (2019) 189–195.
[23] L. Zang, H. He, Q. Xu, Y. Yu, N. Zheng, W. Liu, T. Hayashi, S.I. Tashiro, S. Onodera, T. Ikejima, Reactive oxygen species H_2O_2 and center dot OH, but not O-2 center dot (-) promote oridonin-induced phagocytosis of apoptotic cells by human histocytic lymphoma U937 cells, Int. Immunopharmacol. 15 (2013) 414–423.
[24] B. Beutler, Innate immunity: an overview, Mol. Immunol. 40 (2004) 845–859.
[25] G.M. Rosen, S. Pou, C.L. Ramos, M.S. Cohen, B.E. Britigan, Free radicals and phagocytic cells, FASEB J. 9 (1995) 200–209.
[26] S.J. Chanock, J. Elbenna, R.M. Smith, B.M. Babior, The respiratory burst oxidase, J. Biol. Chem. 269 (1994) 24519–24522.
[27] C.A.K. Kalgraff, H.I. Wergeland, E.F. Pettersen, Flow cytometry assays of respiratory burst in Atlantic salmon (Salmo salar L.) and in Atlantic cod (Gadus morhua L.) leucocytes, Fish Shellfish Immunol. 31 (2011) 381–388.
[28] M. Guo, X. Tang, X. Sheng, J. Xing, W. Zhan, The immune adjuvant effects of flounder (*Paralichthys olivaceus*) interleukin-6 on *e. tarda* subunit vaccine OmpV, Int. J. Mol. Sci. 18 (2017).
[29] J. Xing, Y. Chang, X. Tang, X. Sheng, W. Zhan, Separation of haemocyte subpopulations in shrimp *Fenneropenaeus chinensis* by immunomagnetic bead using monoclonal antibody against granulocytes, Fish Shellfish Immunol. 60 (2017) 114–118.
[30] Q. Li, W. Zhan, J. Xing, X. Sheng, Production, characterisation and applicability of monoclonal antibodies to immunoglobulin of Japanese flounder (*Paralichthys olivaceus*), Fish Shellfish Immunol. 23 (2007) 982–990.
[31] Y. Cui, Z. Wei, Y. Shen, C. Li, Y. Shao, W. Zhang, X. Zhao, A novel C1q-domain-containing protein from razor clam Sinonovacula constricta mediates G-bacterial agglutination as a pattern recognition receptor, Dev. Comp. Immunol. 79 (2018) 166–174.
[32] L. Vidard, M. Kovacsovics-Bankowski, S.K. Kraeft, L.B. Chen, B. Benacerraf, K.L. Rock, Analysis of MHC class II presentation of particulate antigens of B lymphocytes, J. Immunol. 156 (1996) 2809 LP-2818.
[33] D. Parra, A.M. Rieger, J. Li, Y.A. Zhang, L.M. Randall, C.A. Hunter, D.R. Barreda, J.O. Sunyer, Pivotal Advance: peritoneal cavity B-1 B cells have phagocytic and microbicidal capacities and present phagocytosed antigen to CD4+ T cells, J. Leukoc. Biol. 91 (2012) 525–536.
[34] L. Zhu, A. Lin, T. Shao, L. Nie, W. Dong, L. Xiang, J. Shao, B cells in teleost fish act as pivotal initiating APCs in priming adaptive immunity: an evolutionary perspective on the origin of the B-1 cell subset and B7 molecules, J. Immunol. 192 (2014) 2699–2714.
[35] J. Agier, J. Pastwińska, E. Brzezińska-Błaszczyk, An overview of mast cell pattern recognition receptors, Inflamm. Res. 67 (2018) 1–10.
[36] A. Spittler, C. Schiller, M. Willheim, C. Tempfer, S. Winkler, G. Boltznitulescu, IL-10 augments CD23 expression on U937 cells and down-regulates IL-4-driven CD23 expression on cultured human blood monocytes: effects of IL-10 and other cytokines on cell phenotype and phagocytosis, Immunology 85 (1995) 311–317.
[37] G. Sellge, T.A. Kufer, PRR-signaling pathways: learning from microbial tactics, Semin. Immunopathol. 27 (2015) 75–84.
[38] Y.J. Li, Y.L. Li, X.C. Cao, X.Y. Jin, T.C. Jin, Pattern recognition receptors in zebrafish provide functional and evolutionary insight into innate immune signaling pathways, Cell. Mol. Immunol. 14 (2016) 80–89.
[39] Z. Lv, Z. Wei, Z. Zhang, C. Li, Y. Shao, W. Zhang, X. Zhao, Y. Li, X. Duan, J. Xiong, Characterization of NLRP3-like gene from Apostichopus japonicus provides new evidence on inflammation response in invertebrates, Fish Shellfish Immunol. 68 (2017) 114–123.
[40] Z. Lv, Z. Zhang, Z. Wei, C. Li, Y. Shao, W. Zhang, X. Zhao, J. Xiong, HMGB3 modulates ROS production via activating TLR cascade in Apostichopus japonicus, Dev. Comp. Immunol. 77 (2017) 128–137.

[41] R. Nakamura, A. Sene, A. Santeford, A. Gdoura, S. Kubota, N. Zapata, et al., IL10-driven STAT3 signalling in senescent macrophages promotes pathological eye angiogenesis, Nat. Commun. 6 (2015) 7847.
[42] B. Koscsó, B. Csóka, E. Kókai, Z.H. Németh, P. Pacher, L. Virág, et al., Adenosine augments IL-10-induced STAT3 signaling in M2c macrophages, J. Leukoc. Biol. 94 (2013) 1309–1315.
[43] J.H. Xu, H. Ao, J.Q. Hong, J.Y. Zhou, Y.J. Weng, J.D. Zhang, et al., Paeoniflorin inhibits lipopolysaccharide-induced microglia inflammation and phagocytosis through IL-10-STAT3 signaling pathway, J. Biochem. Mol. Biol. 33 (2017) 169–175.
[44] L. Shi, H. Zheng, W. Hu, B. Zhou, X. Dai, Y. Zhang, Z. Liu, X. Wu, C. Zhao, G. Liang, Niclosamide inhibition of STAT3 synergizes with erlotinib in human colon cancer, OncoTargets Ther. 10 (2017) 1767–1776.
[45] R. Li, Z. Hu, S.Y. Sun, Z.G. Chen, T.K. Owonikoko, G.L. Sica, S.S. Ramalingam, W.J. Curran, F.R. Khuri, X. Deng, Niclosamide overcomes acquired resistance to erlotinib through suppression of STAT3 in non-small cell lung cancer, Mol. Cancer Ther. 12 (2013) 2200–2212.
[46] X. Ren, L. Duan, Q. He, Z. Zhang, Y. Zhou, D. Wu, J. Pan, D. Pei, K. Ding, Identification of niclosamide as a new small-molecule inhibitor of the STAT3 signaling pathway, ACS Med. Chem. Lett. 1 (2010) 454–459.